ULTRASONIC CHARACTERIZATION OF CYLINDRICAL POROSITY

- A MODEL STUDY

Satish M. Nair, David K. Hsu, and James H. Rose

Center for NDE
Iowa State University
Ames, IA 50011

INTRODUCTION

Recently, the frequency dependent ultrasonic attenuation has been used to find the volume fraction and pore size of gas porosity in cast aluminum alloys [1,2]. The question arises as to whether these techniques can be adapted for the characterization of porosity in layered materials, such as graphite-epoxy composites. One major difference lies in the morphology of the pores: they are nearly spherical in the aluminum alloys whereas they are long, parallel and needle-like in graphite-epoxy [3]. Consequently, it is of considerable interest to adapt the techniques developed for porosity estimation in [1] for the study of a collection of needle-like pores which we model as cylindrical voids.

In this paper, we present an experimental/theoretical study of the possibility of estimating the volume fraction of pores with cylindrical shapes. The structure of the paper is as follows. First, the total scattering cross-sections for a longitudinal wave incident normally on long cylindrical cavities are obtained. The cross-sections are computed from standard expressions for right circular and elliptic cylinders. For the latter, a simple technique reducing the complexity of the computation is developed. The scattering cross-sections are then used to estimate the attenuation in solids containing a random distribution of long, cylindrical voids. This is compared with the results obtained from measurements made on aluminum blocks, with randomly placed through drilled parallel holes. Next, a new method for estimating the volume fraction from the ultrasonic attenuation is introduced. Finally, the application of the model to studying the porosity in graphite-epoxy composites is discussed.

A major extension of previous methods lies in the proposed technique of estimating the volume fraction from the attenuation. As discussed below, the volume fraction is found to be directly proportional to the attenuation slope, which is obtained by fitting a linear dependence to the attenuation in the intermediate 'ka' range. This new method will be found useful in composite materials, where the attenuation is often found to be nearly linear with respect to frequency in a broad range.

ULTRASONIC ATTENUATION DUE TO CYLINDRICAL PORES

Gubernatis and Domany [4] have shown that for dilute volume fractions, the ultrasonic attenuation for spherical pores can be computed from

$$\alpha \simeq \frac{1}{2} \sum_{i=1}^{N} n_i \gamma_i(a_i,k) \qquad (1)$$

where n_i is the number of voids of radius a_i per unit volume and γ_i is the total scattering cross-section of voids having a radius a_i. N is the total number of void sizes, $a_1 \ldots a_N$, in the porous media. Equation (1) makes the assumption that there is no correlation between individual scatterers. By considering the loss in energy of an ultrasonic beam through the porous solid, Eq. (1) has also been derived by Martin [5].

Equation (1) is adopted as the basis for computing the attenuation of ultrasound by infinitely long cylindrical pores. In this case, n_i is interpreted as the number of voids per unit cross-sectional area and γ_i the total scattering cross-section per unit length. The values of γ_i are hence required for the computation. The cross-sections for right circular cylinders are reported in sub-section A. A new method for computing the cross-sections for elliptic cylindrical cavities is discussed in sub-section B. Finally, in sub-section C, the estimated attenuation from Eq. (1) is compared with experiment.

Scattering Cross-Section for a Circular Cylindrical Cavity

The total scattering cross-section is defined as the scattered energy in all directions per unit time per unit intensity of the beam. Methods of computing the total scattering cross-section per unit length γ for an infinitely long circular cylindrical cavity are given in Refs. 6 and 7. It is seen that γ depends on the ratio of the shear to longitudinal velocity, $\eta = V_S/V_L$, and ka, which is the product of the longitudinal wave number k and the radius of the cavity a.

The reduced scattering cross-section Γ is defined as the total scattering cross-section divided by the geometric cross-section and for an infinitely long cylinder implies

$$\gamma(ka,\eta) = \Gamma(ka,\eta) \times 4a \qquad (2)$$

It is dependent on the host medium only through the Poisson's ratio which is fixed by η. The reduced scattering cross-sections for $0.4<\eta<0.6$ are shown in Fig. 1. The reduced scattering cross-section is seen to have a nearly constant value at high frequencies $ka \gg 1$ and rises monotonically as k^3 for low frequencies. For small values of η, Γ is characterized by a peak in the intermediate ka regime. As the values of η become larger, the peak moves to higher values of η. Since most structural solids have a value of η nearly equal to 0.5, this peak is not visible in most investigations.

Scattering Cross-Section for an Elliptic Cylindrical Cavity

The integral equation for the particle displacement ϕ, associated with a harmonically time-varying disturbance, u^{in}, incident on a long cylindrical cavity in an isotropic elastic medium is given by [8]

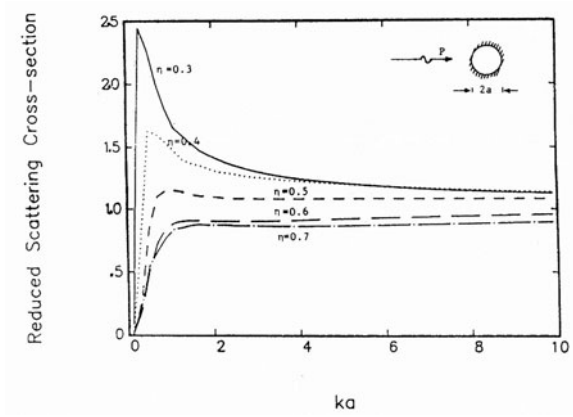

Fig. 1. Reduced scattering cross-section $\Gamma(ka)$ for a circular cylindrical cavity for various ratios of shear to longitudinal velocities ($\eta=V_S/V_L$).

$$-\frac{1}{2}\phi_\gamma(\underline{x}_p) + \int_C \tau^{\Gamma}_{\alpha\beta\gamma}(\underline{x},\underline{x}_p)n_\beta(\underline{x})\phi_\alpha(\underline{x})ds = -u^{in}_\gamma(\underline{x}_p) \text{ when } \underline{x}_p \varepsilon C \quad (3)$$

Here $\tau^{\Gamma}_{\alpha\beta\gamma}$ is the 2-dimensional Green's tensor, C is the boundary of the cavity and n_β is the unit outward normal vector to C. For cases where the boundary of the cavity is specified by an ellipse, Eq. (3) can be simplified by using elliptic cylindrical coordinates and can be written as

$$-\frac{1}{2}\phi_\gamma(\tilde{\eta}_p) + \int_0^{2\pi} \tau^{\Gamma}_{\alpha\beta\gamma}(\tilde{\eta},\tilde{\eta}_p)n_\beta(\tilde{\eta})\phi_\alpha(\tilde{\eta})s(\tilde{\eta})d\tilde{\eta} = -u^{in}_\gamma(\tilde{\eta}_p) \quad (4)$$

Here, $\tilde{\eta}$ refers to one of the elliptic cylindrical coordinates. $s(\tilde{\eta})$ is related to the semi-major axis 'b' and semi-minor axis 'a' by

$$s(\tilde{\eta}) = (a^2\sin^2\tilde{\eta} + b^2\cos^2\tilde{\eta}) \quad (5)$$

For an incident P wave, specified by

$$\underline{u}^{in} = \underline{U}^{P} \exp(ik\hat{\underline{\alpha}}\cdot\underline{x}) \tag{6}$$

Equation (4) is solved for the particle displacements 'ϕ' on the surface of the ellipse. These are then used to compute the scattering cross-sections from [8]

$$\gamma(k,\frac{b}{a},b,\eta) = \frac{1}{k}\,\mathrm{Im}\left[\frac{\underline{U}^{P*}\cdot\underline{\chi}^{P}(\hat{\underline{\alpha}})}{\underline{U}^{P}\cdot\underline{U}^{P*}}\right] \tag{7}$$

where

$$\underline{\chi}^{P}(\hat{\underline{\alpha}}) = \frac{-ik}{\lambda+2\mu}\,\hat{\underline{\alpha}}\int_{0}^{2\pi}\{\lambda(\underline{u}^{sc}\cdot\underline{n})+2\mu(\underline{u}^{sc}\cdot\hat{\underline{\alpha}})(\hat{\underline{\alpha}}\cdot\underline{n})\}\ \exp(ik\hat{\underline{\alpha}}\cdot\underline{x})s(\tilde{\eta})d\tilde{\eta} \tag{8}$$

The reduced scattering cross-section Γ is defined by

$$\gamma = \Gamma \times 4b \tag{9}$$

Figure 2 shows the reduced scattering cross-sections for various aspect ratios (b/a's) when a P wave is incident normal to the cylindrical and semi-major axis. The dependence of the reduced cross-section Γ on b/a is most apparent at low and intermediate frequencies. As can be seen, a peak develops near ka = 0.8 as b/a ranges from 1 (a right circular cylinder) to 20 (nearly a ribbon crack). Consequently, pores with greater eccentricity in this orientation will attenuate ultrasound more efficiently and will have a larger attenuation slope.

The computer program is checked by computing various known scattering cross-sections. Figure 3 shows a comparison between the scattering cross-sections computed from the exact relation (2) and the boundary-integral equation as implemented in Eqs. (3)-(8) for a right circular cylinder. In the limiting case when $b/a \to \infty$, the elliptical cylinder will take the form of a flat ribbon crack. A comparison between the scattering cross-sections for a flat ribbon crack, obtained exactly in [9], and that obtained by using a large b/a ratio (b/a=20) in Eq. (7) is also depicted in Fig. 3. In both cases, it is seen that the boundary integral results are in good agreement with the exact results, thus confirming the correctness of the computer code.

Experimental Verification

The computer scattering cross-sections for circular and elliptical cylindrical cavities are substituted in Eq. (1) to estimate the attenuation due to cylindrical voids in an isotropic host. Aluminum blocks are chosen as the host medium. Small holes are drilled from one face to the other, to simulate porosity. The ultrasonic attenuation is measured in an immersion tank using a through-transmission set-up, with two 1/4" diameter 5MHz broadband transducers. The transducers are aligned and oriented such that the insonifying ultrasonic beam is perpendicular to both the sample surfaces and the axis of the holes. The samples are taped so that the holes are filled with air during the immersion measurements. The specimens are polished flat so that surface roughness does not contribute to the measured attenuation. Signals through the

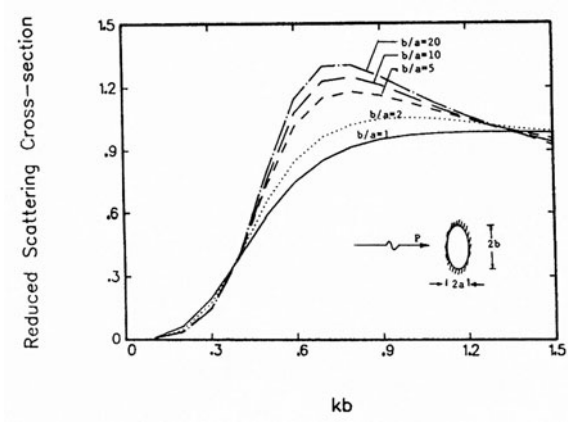

Fig. 2. Reduced scattering cross-section $\Gamma(ka)$ for elliptic cylindrical cavities having a variety of aspect ratios (b/a's) and for η=0.56.

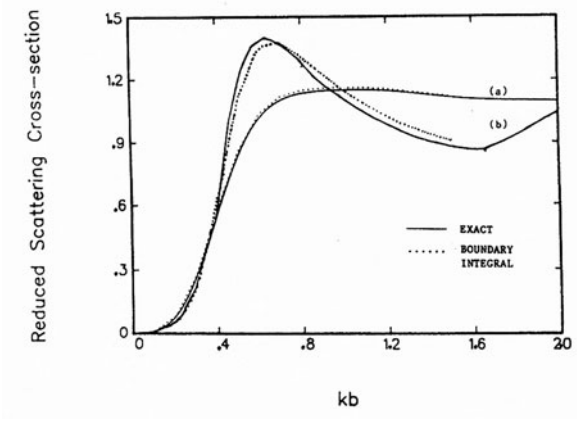

Fig. 3. Comparison between the reduced cross-sections obtained from a boundary-integral approach and by using exact solutions;a) for a circular cylindrical cavity, (b) for a flat ribbon crack.

"porous" samples are deconvolved with the signal through a blank sample without any holes to measure the attenuation due to porosity alone. Spatial averaging over the whole width of the sample is carried out to account for the randomness in hole locations. Details of the aluminum blocks used for verification are given below:

Sample 1: 1.065" x 0.488" x 0.474"
26 holes of 0.02" diameter
Void volume fraction = 1.64%

Sample 2: 1.149" x 0.488" x 0.508"
14 and 13 holes of 0.02" and 0.031" diameter, respectively
Void volume fraction = 3.09%

Figures 4(a) and (b) show a comparison of the computed attenuation and the attenuation measured experimentally. In both figures, it is seen that the experimentally measured attenuation is slightly larger than the attenuation predicted by the model. The source of the discrepancy is unknown.

ATTENUATION SLOPE AND VOLUME FRACTION

The attenuation due to dilute porosity in solids (such as gas porosity in cast aluminum alloys) shows a power law behavior with frequency in the ka<<1 region and a frequency independent plateau for ka>>1. The transition between these two regions in the intermediate ka regime may be approximated by a linear frequency dependence. The slope of the attenuation with respect to frequency in this region is denoted as the "attenuation slope". The attenuation slope has been widely used for tissue characterization in biomedical ultrasonics [10]. Here, it is

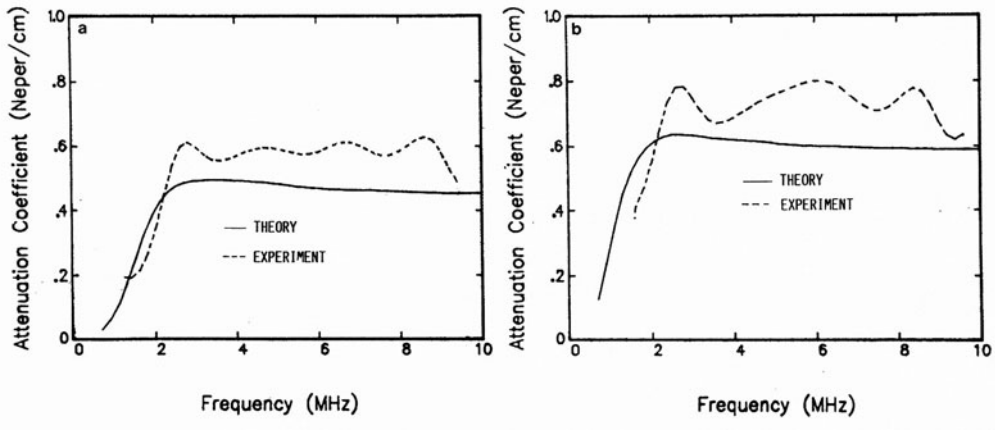

Fig. 4. Comparison of the theoretically estimated attenuation with that measured in an aluminum block (a) containing 1.64% porosity, (b) containing 3.09% porosity.

shown that the attenuation slope can be directly related to the porosity volume fraction through material constants. It is found that the above relationship holds for both spherical and cylindrical voids; the proportionality constants, however, are different.

The scattering cross-section is approximated in the intermediate 'ka' regime by a first order Taylor's series expansion about the inflection point of the curve. It is then expressed as

$$\gamma(ka) = [\Gamma(k_o a_o) + \Gamma'_{cc}(k_o a_o) \times (ka - k_o a_o)] \times 4a \qquad (10)$$

Here $k_o a_o$ represents the inflection point about which the expansion is carried out and Γ'_{cc} is the slope of the approximately linear region of the reduced scattering cross-section with ka. Substituting Eq. (10) in Eq. (1) and taking the derivative with respect to frequency, we have

$$\frac{d\alpha}{df} \simeq \frac{4\Gamma'_{cc}}{V_L} \sum_{i=1}^{N} n_i \pi a_i^2$$

Here, V_L is the longitudinal wave velocity in the material.

Therefore, the porosity volume fraction given by

$$c = \sum_{i=1}^{N} n_i \pi a_i^2 \qquad (12)$$

is related to the attenuation slope by

$$c \simeq \frac{V_L}{4\Gamma'_{cc}} \times \frac{d\alpha}{df} \qquad (13)$$

Since V_L and Γ'_{cc} are material constants, it is seen that the porosity volume fraction can be estimated directly from the attenuation slope. In particular, it is noted that this estimation of the porosity volume fraction does not depend explicitly on the pore size or its distribution.

For solids containing spherical voids instead of cylindrical holes, a similar derivation can be carried out. It is seen that the pore volume fraction 'c' is again directly related to the attenuation slope by material constants and can be estimated from the relation

$$c \simeq \frac{2V_L}{3\pi\Gamma'_{sp}} \times \frac{d\alpha}{df} \qquad (14)$$

Here Γ'_{sp} is the slope at the inflection point of the reduced scattering cross-section for a spherical void with respect to ka. For Al, V_L=0.632 cm/μs, Γ'_{sp}=2.031 and the relationship between the volume fraction and attenuation slope is therefore

$$c\ (\%) = 6.603\ \frac{d\alpha}{df}\ (\text{Np/cm MHz}) \qquad (15)$$

Equations (13) and (14) can be used to estimate pore volume fractions from the experimentally measured attenuation. In the aluminum blocks containing cylindrical holes, the holes are not small enough to have a wide range of frequencies over which the attenuation is linear. Hence, it is not possible to confidently provide a linear fit to the measured attenuation in this narrow, low frequency range.

However, this problem does not exist for the published data on gas porosity in aluminum. In this case, the bandwidth is more than adequate. It is seen that the algorithm successfully predicts volume fractions of gas porosity in these castings. Estimates using Eq. (15) are compared with those made by using the Kramers-Kronig relations and values obtained by weight measurements [1]. This comparison is represented graphically in Fig. 5. As seen, Eq. (15) is quite successful in predicting the volume fraction and is comparable with the other methods.

APPLICATION TO COMPOSITES

Consider a fully compacted composite laminate, with a uni-directional lay-up. If the fibers are randomly located in the resin matrix, the laminate can be considered as being effectively homogeneous. In such a case, the plane perpendicular to the fiber axis is a plane of isotropy. A uni-directional composite laminate can hence be idealized as a transversely-isotropic solid.

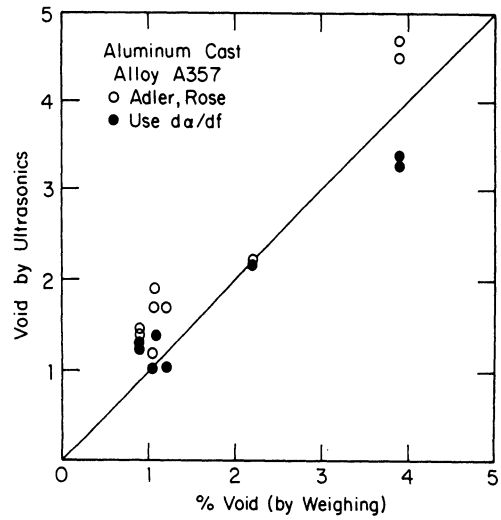

Fig. 5. Comparison of porosity volume fraction estimates made by using "attenuation slope" with other methods.

The stiffness matrix for a 3-D transversely-isotropic solid is characterized by 5 independent constants. A morphological study of porosity in composites [3] indicates that the pores are interlaminar and tend to be oriented in the fiber directions. The pore dimensions along the fiber directions are, in general, much larger than the cross-sectional dimensions. It is seen that the pores are best approximated as long, elliptic cylindrical cavities. Under such an assumption, if the incident wave is perpendicular to the fiber axis, the study of the scattering from the pores reduces to a plane strain problem. The stress-strain relations are now characterized by only two independent material constants and can be mapped onto the stress-strain relations of an isotropic material. The scattering cross-sections for the pores are obtained in the same way as for isotropic mateirals.

Image analyses data from photomicrographs of the cross-sections of two unidirectional graphite-epoxy laminates, containing 2.04% and 1.14% porosity, respectively, are used to obtain the individual pore characteristics. The scattering cross-sections for each pore is computed using Eq. (7). These are then substituted in Eq. (1) to estimate the attenuation in the two laminates. The attenuation estimated above is compared with the experimentally measured attenuation and is shown in Fig. 6(a) and (b). The large discrepancy between the measured and calculated attenuation probably comes about from the various approximations incorporated in the computation (neglecting the layered nature of the solid, no correlation among scatterers, infinitely long voids, approximating the cross-sectional shape by a smooth ellipse). The non-uniformity of the pore distribution is probably a contributing factor since the attenuation is measured at a different location from where the image analyses samples are cut. However, it is interesting to note that both exhibit the same kind of linear behavior with frequency and have the same order of magnitude.

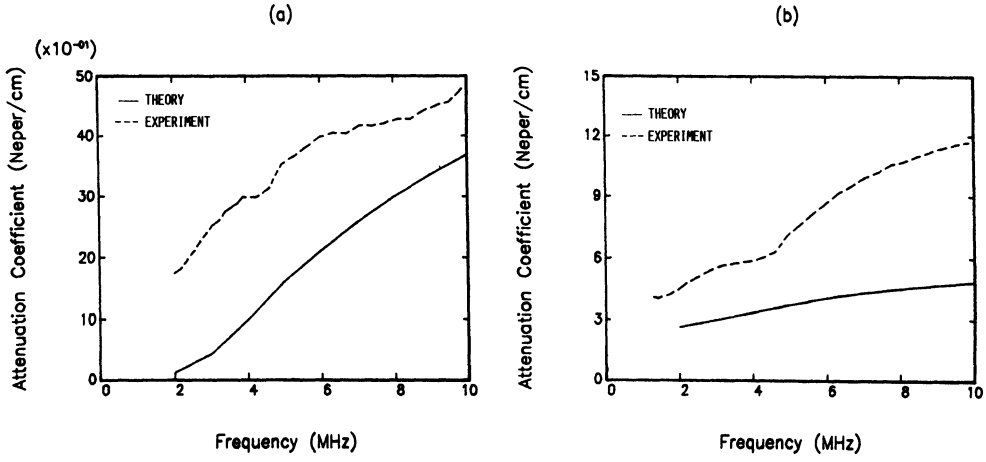

Fig. 6. Comparison of the theoretically estimated attenuation with that measured experimentally in a uni-directional GR/EP composite (a) containing 1.14% porosity, (b) containing 2.04% porosity.

SUMMARY

In an effort to characterize the porosity in graphite-epoxy composites, models containing long, cylindrical holes are studied. The ultrasonic attenuation in such models is estimated from the scattering cross-sections of the holes and then verified experimentally. A simple algorithm relating the attenuation slope in the intermediate "ka" regime and the porosity volume fraction is developed. The algorithm is successfully applied in estimating the volume fractions of gas porosity in aluminum alloy castings.

Under the assumption that the pores in graphite-epoxy composites can be approximated as long cylinders, data from the image analyses of photomicrographs are used to predict the attenuation in some of the uni-directional composite specimens. Comparisons with the experimentally measured attenuation suggest that the attenuation slope algorithm may be successfully used in estimating the porosity volume fractions in graphite-epoxy composites [11].

ACKNOWLEDGEMENT

This work is supported by the NSF university/industry Center for NDE at Iowa State University. The authors would like to thank R. A. Roberts for discussions.

REFERENCES

1. L. Adler, J. H. Rose, and C. Mobley, "Ultrasonic method to determine gas porosity in aluminum alloy castings: Theory and experiment", J. Appl. Phys., Vol. 59, No. 2, 1986, pp. 336-347.
2. J. H. Rose, D. K. Hsu, and L. Adler, "Ultrasonic characterization of porosity using the Kramers-Kronig relations", J. de Physique. Colloque C10 Supp. au n° 12, Tome 46, C10-787 to C10-790, 1985, and J. H. Rose, "Kramers-Kronig relations and the ultrasonic characterization of porosity", Review of Progress in Quantitative NDE, 5B, D. O. Thompson and D. E. Chimenti, Eds., (Plenum Press, NY, 1986), pp. 1617-1623.
3. D. K. Hsu and K. M. Uhl, "A morphological study of porosity defects in graphite-epoxy composites", these proceedings.
4. J. E. Gubernatis and E. Domany, "Effects of microstructure on the speed and attenuation of elastic waves: Formal theory and simple approximations", Review of Progress in Quantitative NDE, 2A, D. O. Thompson and D. E. Chimenti, Eds., (Plenum Press, NY, 1983), pp. 833-850.
5. B. G. Martin, "Ultrasonic attenuation due to voids in fibre-reinforced materials", NDT International, October 1986, pp. 242-246.
6. T. S. Lewis, D. W. Kraft, and N. Hom, "Scattering of elastic waves by a cylindrical cavity in a solid", J. Appl. Phys., vol. 47, No. 5, 1976, pp. 1795-1798.
7. Y. H. Pao and C. C. Mow, "Diffraction of elastic waves and dynamic stress concentrations", Crane and Russak, New York, 1973.
8. T. H. Tan, "Diffraction theory for time-harmonic elastic waves", Ph.D. Thesis, Delft Univ. of Technology, Netherlands, Nov. 1975.
9. J. H. M. T. van der Hijden and F. L. Neerhoff, "Scattering of elastic waves by a plane crack of finite width", ASME Journal of Applied Mechanics, Vol. 51, 1984, pp. 646-651.
10. P. H. Johnston, "Phase-insensitive detection and the method of moments of ultrasonic tissue characterization", Ph.D. Thesis, Washington University, Missouri, August 1985.
11. D. K. Hsu and S. M. Nair, "Evaluation of porosity in graphite-epoxy composites by frequency dependence of ultrasonic attenuation", these proceedings.